



USDOT Tier 1  
University Transportation Center  
on Improving Rail Transportation  
Infrastructure Sustainability and Durability

Final Report UNLV-4

**DEVELOPMENT OF A PLATFORM TO ENABLE REAL TIME, NON-DISRUPTIVE  
TESTING AND EARLY FAULT DETECTION OF CRITICAL HIGH VOLTAGE  
TRANSFORMERS AND SWITCHGEARS IN HIGH SPEED-RAIL**

By

Ming Zhu, Ph.D.  
Electrical Engineering Laboratory Director  
Department of Electrical and Computer Engineering  
University of Nevada, Las Vegas

and

Yingtao Jiang, Ph.D., Professor  
Department of Electrical and Computer Engineering  
University of Nevada, Las Vegas  
4505 S Maryland Pkwy Box 454026,  
Las Vegas, NV 89154-4026  
yingtao.jiang@unlv.edu

August 2024

Grant Number: 69A3551747132



## **DISCLAIMER**

The contents of this report reflect the views of the authors, who are responsible for the facts and the accuracy of the information presented herein. This document is disseminated in the interest of information exchange. The report is funded, partially or entirely, by a grant from the U.S. Department of Transportation's University Transportation Centers Program. However, the U.S. Government assumes no liability for the contents or use thereof.

## ABSTRACT

Partial discharge (PD) incidents may occur within critical components of high-speed rail electric systems, including transformers, motors, and switchgears. These incidents result from localized defects compromising insulation, unable to withstand electric stress, leading to flashovers. PD propagates and escalates over time, with potentially severe consequences including catastrophic breakdowns, unplanned downtime, and safety hazards. Fortunately, PD activities emit radio frequency (RF) signals, prompting the development of a hardware platform for non-invasive, non-disruptive real-time PD detection and continuous monitoring in high voltage transformers and switchgears within high-speed rail systems.

To achieve continuous and real-time monitoring of PD, the system employs a delicate RF antenna and a high-speed data acquisition system to iteratively scan ambient RF signals across a configurable frequency range (i.e., from 100MHz to 3GHz by default). Intermediate frequency (IF) modulation and sliding frequency windows are utilized to comprehend the broadband RF signals. When RF signals surpass a pre-defined power threshold, the system cassettes these events (i.e., in both time domain raw signal and corresponding spectrum snapshots), ensuring precise detection and trackable records of potential PD occurrences.

In addition to its robust detection capabilities, the system features advanced data management solutions. It streams real-time data and spectrum snapshots to a cloud server, providing seamless and immediate remote accessibility. A dedicated smartphone application has been developed, enabling remote access to the data, thus allowing maintenance teams to monitor and respond to potential issues promptly, regardless of their location.

The system has undergone rigorous testing in laboratory environments, successfully demonstrating its ability to capture RF signals within the specified spectrum accurately. Furthermore, the platform has proven its effectiveness in offering real-time PD inspection and monitoring with remote data accessibility, confirming its potential as a vital tool in enhancing the reliability and safety of high-voltage transformers and switchgears in high-speed rail infrastructure.

Keywords: Partial discharge, real-time monitoring, robust detection, RF signal, broadband signal

## TABLE OF CONTENTS

DISCLAIMER .....	ii
ABSTRACT .....	iii
LIST OF TABLES.....	v
LIST OF FIGURES .....	vi
CHAPTER 1-INTRODUCTION.....	7
1.1 Overview .....	7
1.2 Addressing Partial Discharge in Switchgears and Transformers .....	9
CHAPTER 2 – DEVELOPMENT OF NON-DISRUPTIVE REAL-TIME PD DETECTION AND MONITORING SYSTEM.....	11
2.1 Overview .....	11
2.2 PD Data Acquisition Hardware Platform.....	11
2.3 PD Data Acquisition Process .....	11
2.4 Remote Access to Continuous Real-Time PD Monitoring .....	15
CHAPTER 3 – SYSTEM EVALUATIONS .....	17
3.1 Lab Environment and Hardware Setup .....	17
3.2 Single RF/PD Signal Capturing .....	18
3.3 Dual/Multiple RF/PD Signal Capturing.....	19
3.4 Cloud-Cased Remote Monitoring .....	20
CHAPTER 4 - CONCLUSIONS .....	22
ACKNOWLEDGEMENT .....	22
REFERENCES .....	22
ABOUT THE AUTHORS .....	27

## LIST OF TABLES

Table 1 Key specification of Tektronix RSA 306B real-time RF analyzer.....	11
Table 2 Key specification of the computer for data acquisition.....	11
Table 3 Key specification of the test equipment in the system evaluation.....	17

## LIST OF FIGURES

Figure 1 Conceptual layout traction power substation with 3 high voltage transformers and switchgears ..7	7
Figure 2 Direct drawing of typical section of a traction power facility.....8	8
Figure 3 Causes of PD in switchgears and transformers .....9	9
Figure 4 Damages caused by PD hazards. a) inner surface burn, b) burn through the shield, c) contact damage, d) explosion of the pillar insulator .....9	9
Figure 5 PD signal/data acquisition system.....11	11
Figure 6 Signal capturing, modulation and sampling inside the RSA.....12	12
Figure 7 I/Q modulation for data in time domain.....12	12
Figure 8 RSA API and data flow in computer.....13	13
Figure 9 .r3f and .siq file for data storage.....13	13
Figure 10 .r3f and .siq file manager for data decompression if necessary. ....14	14
Figure 11 a) Iterative sampling and spectrum analysis b) Iteratively scanning to cover the entire PD spectrum.....15	15
Figure 12 IoT-cloud-based remote real-time PD monitoring system diagram.....16	16
Figure 13 Lab test setup for PD DAS (including antenna, RSA 306B, a portable high-performance computer/embedded system), an AWG and 50-ohm resistor (i.e., simulator of PD source), and an oscilloscope.....17	17
Figure 14 Loading program on the PD DAS and get ready for the PD detection and monitoring.....18	18
Figure 15 Capturing signals above the preset power threshold. ....18	18
Figure 16 Capturing 315MHz RF/PD signals a) I/Q ADC values in time domain, b) impulse at 315MHz in frequency domain for one frame, c) impulse at 315MHz in complete scanning iteration .....19	19
Figure 17 Capturing 768MHz RF/PD signals a) I/Q ADC values in time domain, b) impulse at 768MHz in frequency domain for one frame, c) impulse at 768MHz in complete scanning iteration .....19	19
Figure 18 a) No test signal generated (only noises), b) only with a 768MHz generated by AWG, c) only with a Bluetooth signal at about 2400MHz, d) with both 768MHz and Bluetooth signals in the air.....20	20
Figure 19 a) APP login, b) APP access to files, c) File attribute details .....21	21
Figure 20 Email notification of detecting new PD signals .....21	21

# CHAPTER 1-INTRODUCTION

## 1.1 Overview

High-speed rail (HSR) has revolutionized transportation by providing rapid, efficient, and reliable services that connect major cities and regions. The inception of HSR dates back to the 1960s with the launch of Japan's Shinkansen, also known as the "bullet train," which set the benchmark for future developments in the industry (Givoni, 2006). Since then, numerous countries, including France, China, Germany, and Spain, have developed extensive HSR networks, showcasing significant advancements in speed, safety, and passenger comfort (Campos and de Rus, 2009). The California High-Speed Rail (CAHSR) project is also undergoing from Sacramento/San Francisco Bay Area to the Greater Los Angeles/San Deigo (California, 2008; Fox et al., 2008).

The efficient and reliable operation of high-speed rail systems relies heavily on sophisticated high-voltage electrical facilities. Among these, transformers and switchgears play crucial roles in ensuring the seamless transmission and distribution of electrical power necessary for train operations. In HSR systems, transformers are essential for stepping up or stepping down voltage levels to meet the requirements of different stages in the power distribution process (Figure 1 and Figure 2) (Sibal, 2010). They ensure that electrical power is efficiently transmitted from power stations to rail lines, maintaining the correct voltage levels needed for train operations. This step

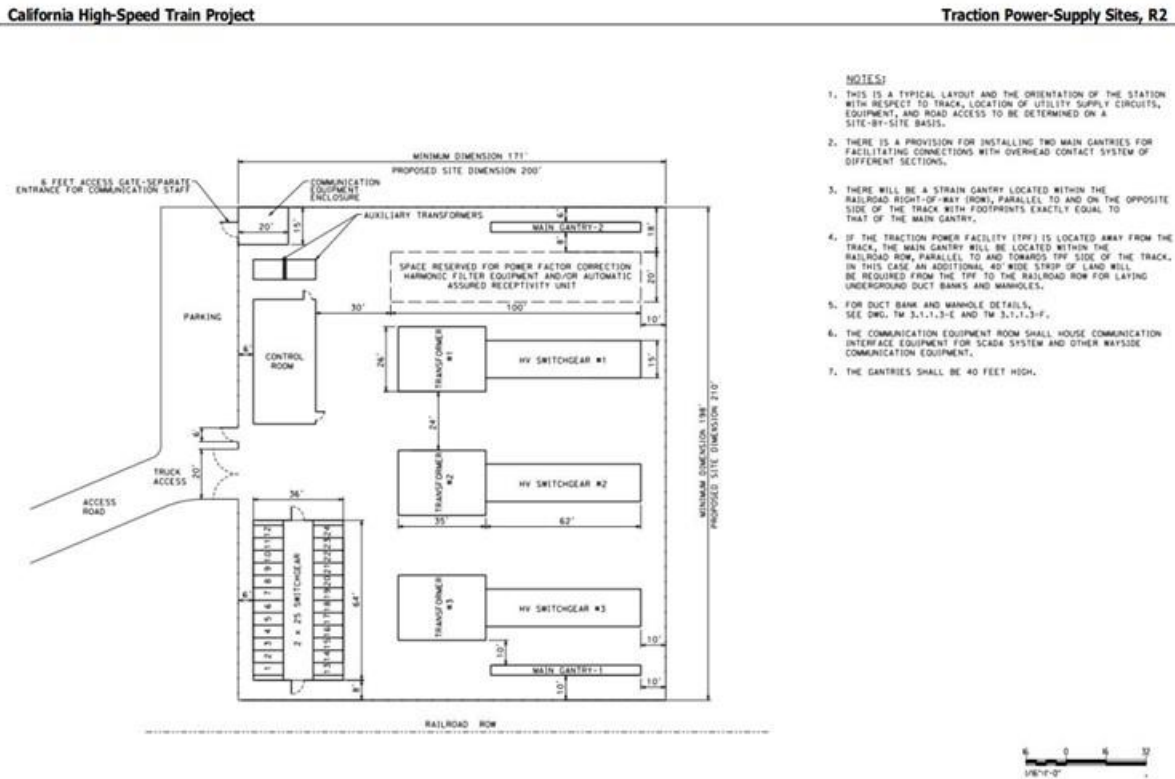


Figure 1 Conceptual layout traction power substation with 3 high voltage transformers and switchgears

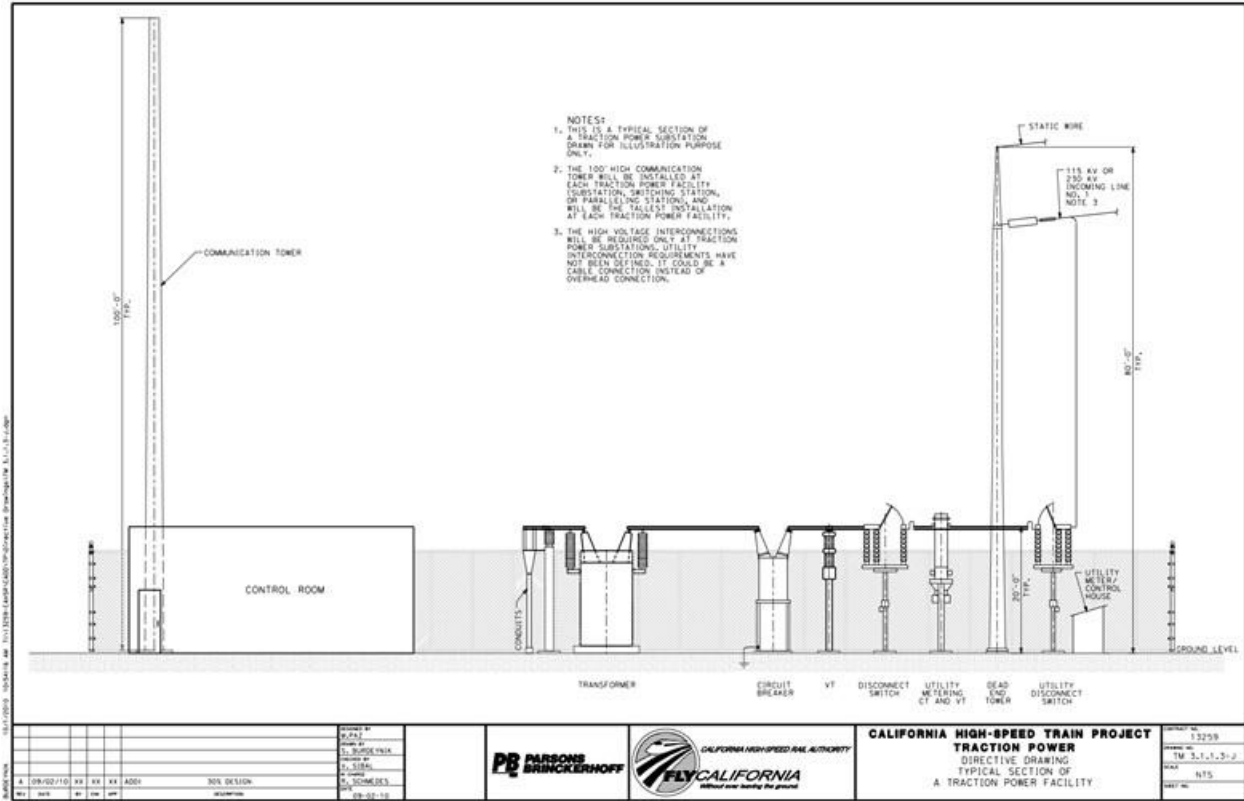


Figure 2 Direct drawing of typical section of a traction power facility

is vital for reducing energy losses and ensuring the smooth functioning of the rail network (Douglas et al., 2015). Switchgears are critical components that control, protect, and isolate electrical circuits within the rail system. They facilitate the safe operation of electrical circuits by managing the flow of electricity, enabling maintenance work, and protecting the system from faults. Switchgears ensure that power distribution remains uninterrupted and safe, even in the event of a fault, thereby maintaining the reliability and safety of high-speed rail operations (Feng et al., 2017). These components are designed to withstand significant electrical stresses and environmental conditions, necessitating robust design and meticulous maintenance. Their effective functioning is crucial for the continuous and safe operation of HSR, which in turn supports the demand for rapid and reliable transportation (IEC, 2014).

However, these high-voltage assets are susceptible to partial discharge (PD), a phenomenon that can significantly undermine their performance and longevity. Partial discharge is a localized dielectric breakdown of a small portion of a solid or fluid electrical insulation system under high voltage stress. PD occurs when the electric field intensity exceeds the dielectric strength of the insulating material, causing localized discharges that do not completely bridge the insulation. These discharges typically result from defects such as voids, cracks, or contaminants within the insulation, which can arise during manufacturing, installation, or due to aging and environmental factors (F.H. Kreuger, 1989). The occurrence of PD in high-voltage transformers and switchgears can have severe consequences. PD generates heat and chemical byproducts that degrade the insulating material over time. This degradation leads to erosion, cracks, and carbonization, progressively weakening the insulation's ability to withstand high voltages (Figure 3). In



transformers, PD can cause insulation failure, leading to costly repairs and significant downtime (Tenbohlen et al., 2017). In switchgears, PD can initiate surface tracking and arcing, which may result in equipment failures and pose fire hazards (Paoletti and Baier, 2001). According to the research (Davies, 2009; Hussain et al., 2016), 85% of high-voltage facility failures and asset damages are due to the PD activities (Figure 4).



Figure 3 Causes of PD in switchgears and transformers

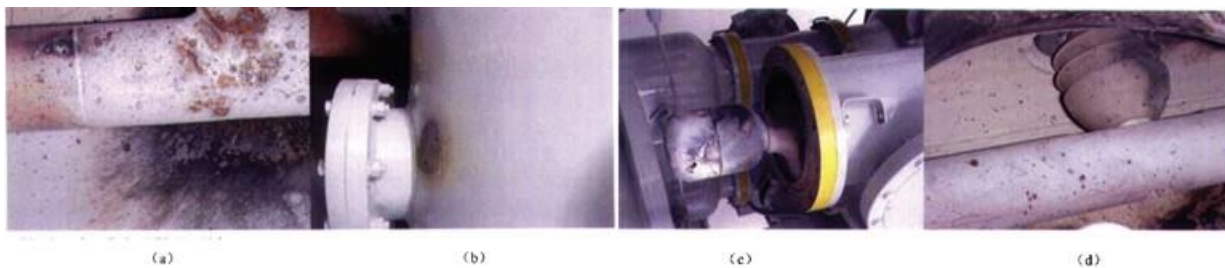


Figure 4 Damages caused by PD hazards. a) inner surface burn, b) burn through the shield, c) contact damage, d) explosion of the pillar insulator

## 1.2 Addressing Partial Discharge in Switchgears and Transformers

To mitigate the risks associated with PD, it is crucial to implement effective monitoring and maintenance strategies. There are multiple approaches to detect PD, such as electromagnetic method (Jahangir et al., 2017; Judd et al., 2005a, 2005b), electrical method (Giussani et al., 2012; IEEE, 2024; Judd, 2011; Timperley, 1983), chemical (Ma et al., 2014; Sheng et al., 2004; Skelly, 2012; Sparkman et al., 2011), acoustic (Kim et al., 2017; Kučera et al., 2019; Qian et al., 2018), optical (Jürgen Fabian et al., 2014; Sarkar et al., 2015) and combinations of these methods (Hauschild and Lemke, 2019; Kim and Hikita, 2013; Kraetge et al., 2013; Yongfen et al., 2015). However, electrical and chemical methods require contact with the equipment, which may bring interference of normal railway operations; whereas acoustic and optical methods may be disrupted by the environmental noises that may affect the detection accuracy. On the other hand, since PD usually emits a radio frequency (RF) signal in a range between 300 and 1500MHz while there lack general background RF signals within this range, we can employ one or multiple ultra-high-frequency (UHF) antenna(s) to scan and detect RF signals in the air within this spectrum. With that, we can obtain a non-invasive/contactless non-disruptive real-time PD detection and monitoring system for high-voltage switchgears and transformers in high-speed rail infrastructure.

To continuously and losslessly monitor PD signals that span over a wide frequency range of 300MHz to 1500MHz, the data acquisition system (DAS) needs a minimum sampling rate of 3GHz (i.e.,  $3 \times 10^9$  samples per second) or higher according to Nyquist Sampling Theory. Correspondingly, the DAS requires high-performance CPU and memories to save and even process this huge amount of data (i.e., approximately 3GB data per second even if using an 8-bit analog-to-digital converter for raw data). Developing such high-speed customized DAQ is usually costly and takes long and to align all hardware to work effectively and reliably. In addition, a single UHF antenna may not suffice the job to constantly capture PD signals of such broadband, and employing multiple antennas will bring extra complexity to the circuit.

To resolve such challenges, we propose to use a single antenna to iteratively scan the spectrum from 100MHz to 2500MHz with intermediate frequency (IF) modulation (Bergmans, 2013; Whitaker, 2017). In this way, the system only has one input and is flexible to various scanning spectrums by adjusting the IF modulation frequencies. One drawback of this method is that the band-limited antenna can only scan a small range of RF spectrum at a time while leaving other spectrum unattended, causing the possibility of missing the PD. Nevertheless, as long as the PD events are repetitive and with proper configuration of the scanning rate, the system will catch PD occurrence confidently.

## CHAPTER 2 – DEVELOPMENT OF NON-DISRUPTIVE REAL-TIME PD DETECTION AND MONITORING SYSTEM

### 2.1 Overview

This chapter introduces the hardware and software platform for PD signal capturing, detection and recording, as well as the cloud-based remote access on the smartphone.

### 2.2 PD Data Acquisition Hardware Platform

We propose a compact and functionally comprehensive and accurate hardware platform as shown in Figure 5. The system only consists of an antenna with a passing bandwidth of 800MHz and center frequency of 136MHz, a Tektronix RSA 306B real-time RF spectrum analyzer (Tektronix, 2015), and a computer (or other high-performance embedded system) with USB-3 interface. Key specifications of the RSA and the computer are listed in

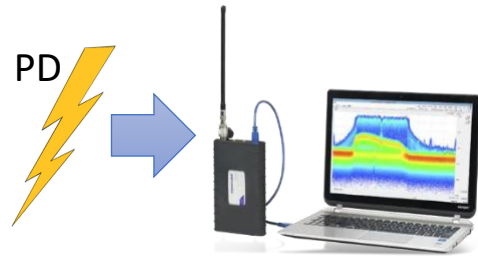


Figure 5 PD signal/data acquisition system

Table 1 and Table 2, respectively.

Table 1 Key specification of Tektronix RSA 306B real-time RF analyzer

Detection Frequency	Sampling Frequency	IF Bandwidth	ADC bit-width	Amplitude Accuracy	Max DC Level	Average Noise
9K – 6.2 GHz	112MSa/s	Max. 40MHz	14-bit	About 1dB	$\pm 40V_{dc}$	$\leq -130dB$

Table 2 Key specification of the computer for data acquisition

CPU	Memory	Interface	Software Support
Intel core i7	16GB DDR4	USB 3	Python and C/C++

### 2.3 PD Data Acquisition Process

During each PD sampling process, the antenna contactlessly senses the PD signals in the air for a certain amount of time (i.e., sample duration, 10 milli-second in this study), and transmits the electric signal to the RSA, which sets up a carrier wave to shift the ultra-high frequency PD signals to a lower spectrum (i.e., intermediate frequency modulation). The IF modulated signal will then

be sampled, quantified and digitized by high-speed analog-to-digital converter (ADC), and the data stream will be transmitted to the computer via USB-3 connection (Figure 6). Here, we call data within one sample duration a data frame or sample frame, and each PD sensing/capturing will generate a frame. The computer reads the data frame via Tektronix application programming interface (API) (Tektronix, 2017), and calculate the data in both time domain in-phase/quadrature (I/Q) stream form (i.e., quadrature modulation) (Figure 7) (Gast, 2005) and spectrum form (Figure 8) using Discrete Fourier Transform (DFT) or Fast Fourier Transform (FFT), Eq. (1). The power is calculated as Eq. (2).

$$X[k] = \sum_{n=0}^{N-1} x(n)e^{-j2\pi kn/N} \quad (1)$$

$$Power = 10 \log \left( \frac{I^2 + Q^2}{1 \text{ mW}} \right) \quad (2)$$

If the system detects any signal power exceeds a pre-set threshold (i.e., -50dB in this study) during each sample frame, the I/Q data and spectrum information of that frame will be recorded.

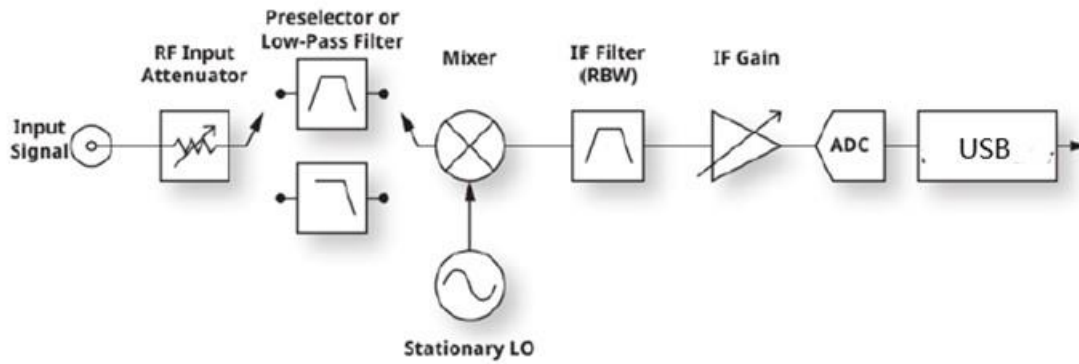


Figure 6 Signal capturing, modulation and sampling inside the RSA

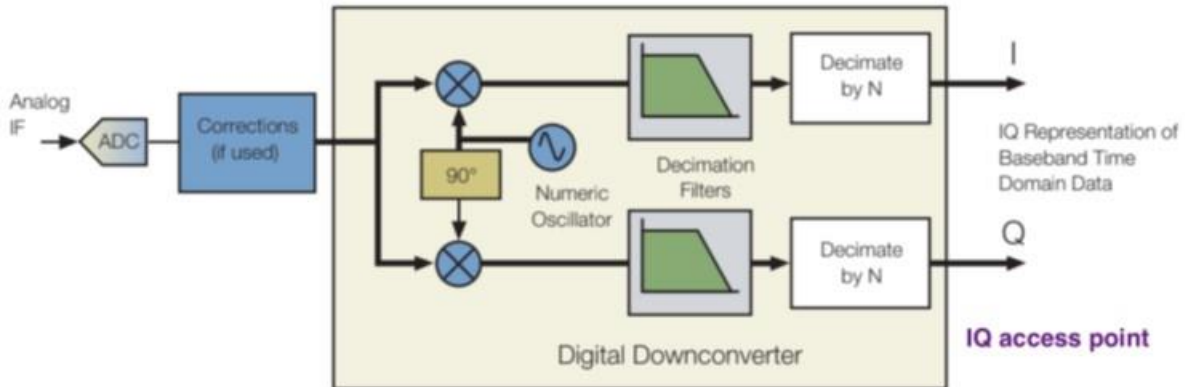


Figure 7 I/Q modulation for data in time domain

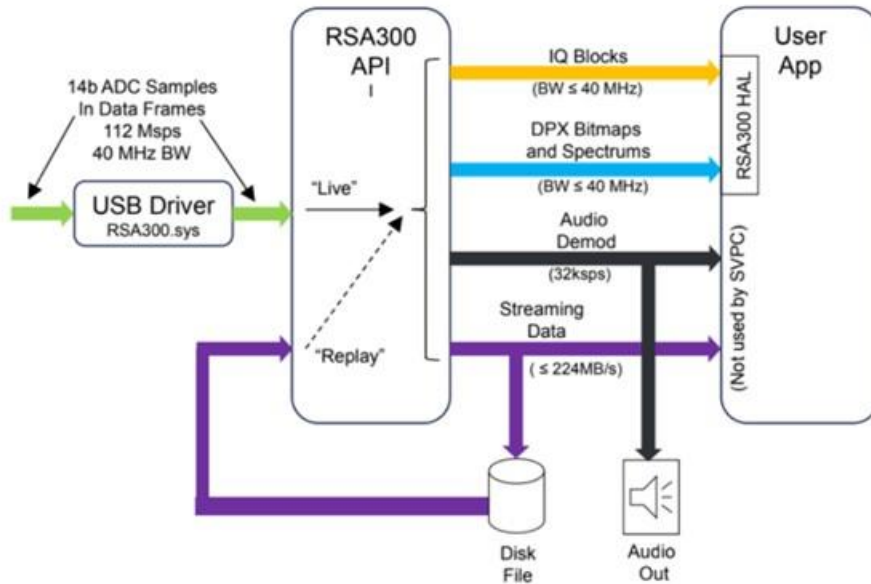


Figure 8 RSA API and data flow in computer

The API produces raw data files for IF and I/Q measurements under .r3f and .siq format (Figure 9), which can be further decoded to .csv file with time sequence but at a cost of much larger file size (Figure 10). The fundamental functions of data acquisition are fulfilled by C/C++ based on RSA 306B API, and a python interface is implemented on top of the C/C++ code and RSA API for the simplicity of user interaction and process control.

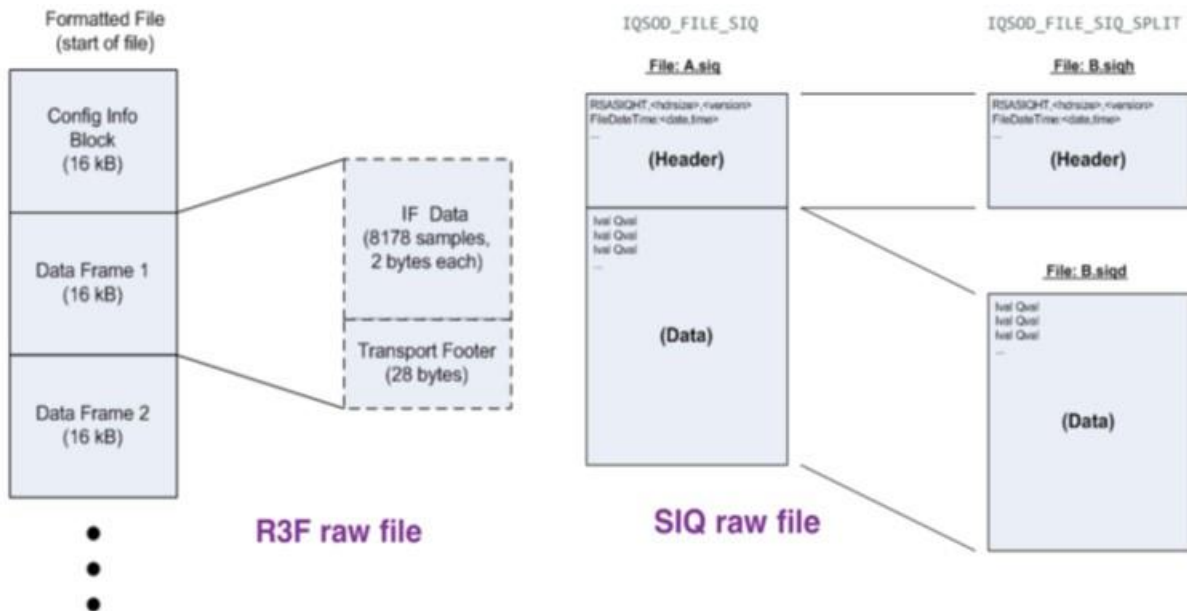


Figure 9 .r3f and .siq file for data storage.

```

class siq_manager_class
{
public :
    common_utility  cutil; // public class instance, by composition, for "common utility" needs
    siq_manager_struct vars; // structured variables for parsing

    siq_manager_class (); // see siq_manager.cpp
    ~siq_manager_class(); // see siq_manager.cpp
    CODE2 clear (); // re-initialize the class member variables, see siq_manager.cpp

    // call to load "*.siq" file and begin processing (user only needs to call this, or the batch version)
    CODE2 load_file
    {
        const char* siq_input,
        const char* output_parsed,
        const char* output_iq,
        bool write_parsed,
        bool write_iq
    };
    CODE2 batch_process_files
    {
        const char* siq_input_directory,
        const char* output_directory,
        std::vector<std::string> input_files_v,
        std::vector<std::string> output_files_v,

```

"siq\_manager\_class"

- Load single SIQ file or batch of files
- Decode bytes of a file
- Process a full text file
- Produce IQ CSV

An instance of "common\_utility" is included by composition for file system management

```

class r3f_manager_class
{
public :
    common_utility  cutil; // public class instance, by composition, for "common utility" needs
    r3f_manager_struct vars; // variables that represent the "*.r3f" file, see r3f_manager_struct.h

    r3f_manager_class (); // r3f_manager.cpp
    ~r3f_manager_class(); // r3f_manager.cpp
    CODE2 clear(); // re-initialize the member variables, see r3f_manager.cpp

    // call to load "*.r3f" file and begin processing (user only needs to call this, or the batch version)
    CODE2 load_file
    {
        const char* r3f_input,
        const char* output_parsed,
        const char* output_equalization,
        const char* output_adc,
        bool write_parsed,
        bool write_equalization,
        bool write_adc
    };
    CODE2 batch_process_files
    {
        const char* r3f_input_directory,
        const char* output_directory,
        std::vector<std::string> input_files_v,
        std::vector<std::string> output_files_v,

```

"r3f\_manager\_class"

- Load single SIQ file or batch of files
- Decode bytes of a file
- Process a full text file
- Produce ADC CSV
- Produce equalization CSV

An instance of "common\_utility" is included by composition for file system management

Figure 10 .r3f and .siq file manager for data decompression if necessary.

As the RSA has the sampling rate of 112MHz and its signal sampling bandwidth of 40MHz, For each complete PD scanning process, the system will iteratively set RSA's IF modulation carrier frequency from 100MHz to 2500MHz (i.e., one iteration), with an incremental step of 40MHz, to cover the PD signal frequency of interest (Figure 11). In the end of each iteration (i.e., 61 samples in 60 iterations of 600 milli-seconds), the system will stitch the power-spectrum diagram of each sample frame for a complete diagram, and remove I/Q data that does not include any PD signals. If any PD signals are captured, the corresponding I/Q data and power-spectrum diagrams will be kept and named according to the timestamp and detected PD frequency. In this way, users can easily observe and trace back the records of PD occurrences, and the system storage can be more efficiently utilized.

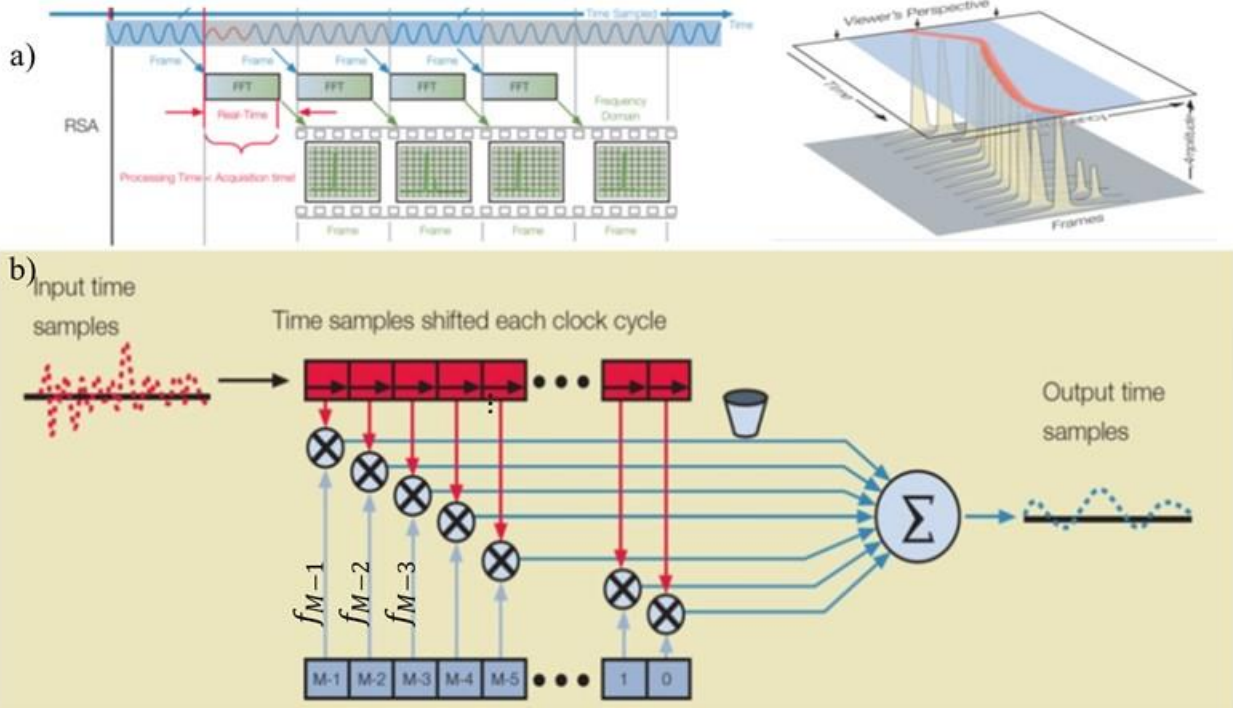


Figure 11 a) Iterative sampling and spectrum analysis b) Iteratively scanning to cover the entire PD spectrum

## 2.4 Remote Access to Continuous Real-Time PD Monitoring

With the expansion of widely spread high-speed rail network, internet of things (IoT) technology should be added to local PD detection and monitoring system at each switchgear/transformer station for the remote accessibility and potentially instant responsiveness to any alert messages it may generate. To achieve this goal, the google cloud service (e.g., Google Drive, Firebase, etc.) is employed and a smartphone application (APP) is developed. The local PD DAS will exploit Rclone (Craig-Wood, 2014) to set up a new cloud storage node, and continuously synchronize the newly detected PD I/Q data and full power-spectrum diagram to the cloud storage at the end of each PD scanning iteration. On the other hand, when the user activates the APP, it will periodically request data synchronization with the cloud server via Google drive API, so that the user can see the updated PD monitoring on their fingertips. In addition, whenever the cloud receives new files, it sends out a notification email to alert the user for newly detected PD events. The overall diagram of this cloud-based remote PD monitoring can be illustrated as Figure 12.

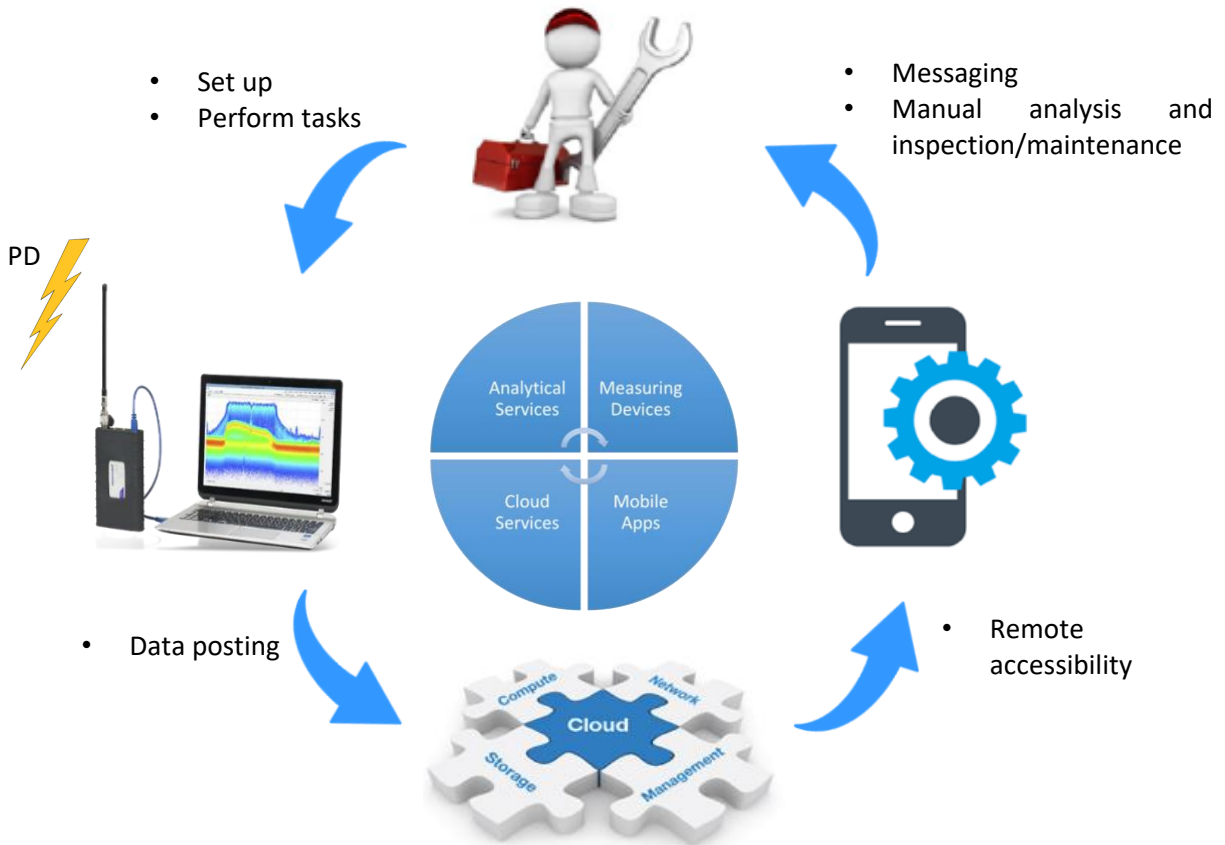


Figure 12 IoT-cloud-based remote real-time PD monitoring system diagram



## CHAPTER 3 – SYSTEM EVALUATIONS

### 3.1 Lab Environment and Hardware Setup

In this chapter, the system evaluation results are presented. The system has been tested under the lab environment (Figure 13), by applying a configurable arbitrary waveform generator (AWG) with a broad bandwidth of 2GHz (BNC, 2021). The AWG output is connected with a 50 $\Omega$  resistive load, which is parallel connected with a 2G bandwidth oscilloscope (Tektronix, 2020) with spectrum analyzer to measure the actual signal waveform, amplitude and frequency that is applied onto the resistor. When the AWG signal passes through the resistor, the circuit generates RF signals as a simulation of PD signals within 100~2500MHz range. Key AWG and oscilloscope specifications are listed in Table 3. Numerical test scenarios have been proceeded, and here we illustrate two representative cases, single signal and dual signals to prove the concept.

Table 3 Key specification of the test equipment in the system evaluation

Equipment	Manufacturer	Model	Bandwidth
AWG	Berkely Nucleonics Corp. (BNC)	685	2 GHz
Oscilloscope	Tektronix	5 Series MSO	2 GHz

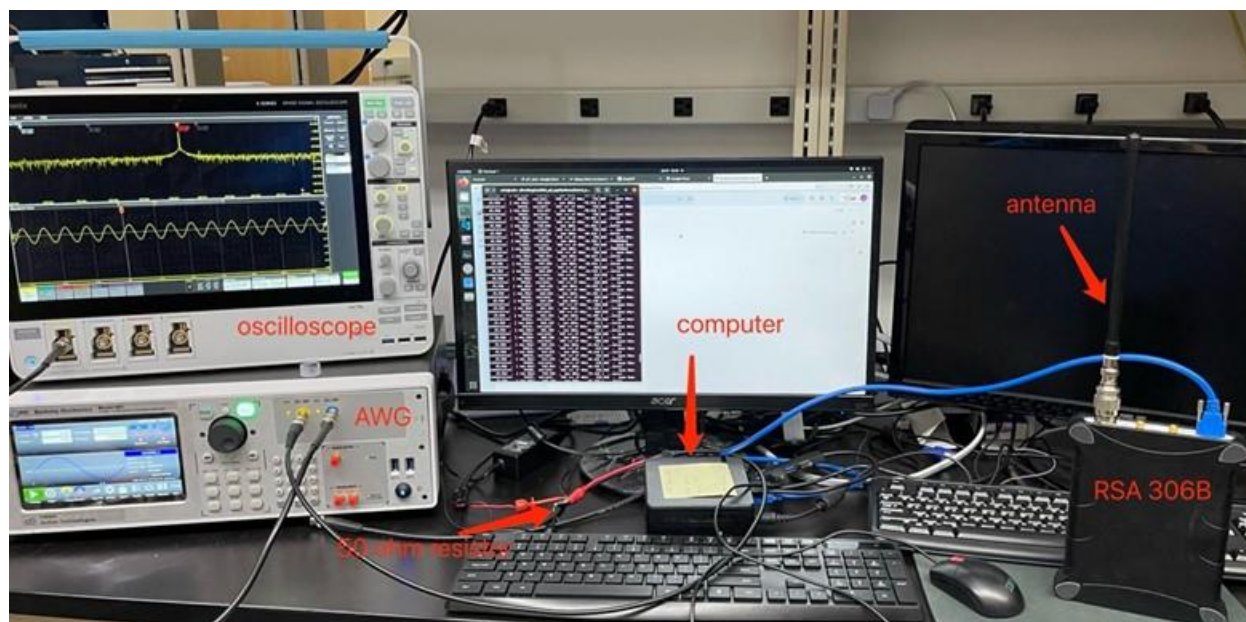
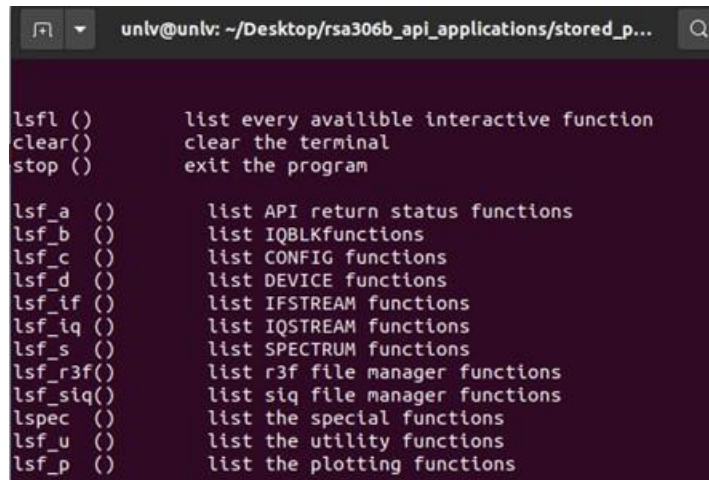


Figure 13 Lab test setup for PD DAS (including antenna, RSA 306B, a portable high-performance computer/embedded system), an AWG and 50-ohm resistor (i.e., simulator of PD source), and an oscilloscope.

### 3.2 Single RF/PD Signal Capturing

We connect the 50Ω resistor with AWG via BNC-alligator cable, and placed the PD DAS with its antenna about one foot away from the resistor. Once the PD DAS is turned on and initiated with the program to scan RF/PD signals in the air (Figure 14), we set up the AWG to generate a 315 MHz sine waveforms of 1V peak-to-peak. Then, the DAS captures the RF signals that exceed the preset threshold (Figure 15), and generates one spreadsheet (i.e., .csv file) of signal value in time-domain (i.e., I/Q ADC values), and a power-spectrum diagram in frequency domain (Figure 16.a and b). In the end of that particular scanning iteration, a complete power-spectrum diagram is drawn from 100MHz to 2500MHz (Figure 16.c). Another test results of 768 MHz RF/PD signal are demonstrated in Figure 17. One can see that although there exist some relatively low frequency noises, most less than 1MHz and -60dB, RF/PD signals of interest can be clearly captured without much interference. In addition, the IF modulation can be observed in Figure 16.a and especially in Figure 17.a, because of the higher IF carrier frequency.



```
unlv@unlv: ~/Desktop/rsa306b_api_applications/stored_p...  
  
lsfl ()      list every available interactive function  
clear()     clear the terminal  
stop ()     exit the program  
  
lsf_a ()    list API return status functions  
lsf_b ()    list IQBLKfunctions  
lsf_c ()    list CONFIG functions  
lsf_d ()    list DEVICE functions  
lsf_if ()   list IFSTREAM functions  
lsf_iq ()   list IQSTREAM functions  
lsf_s ()    list SPECTRUM functions  
lsf_r3f()   list r3f file manager functions  
lsf_siQ()   list siQ file manager functions  
lspec ()    list the special functions  
lsf_u ()    list the utility functions  
lsf_p ()    list the plotting functions
```

Figure 14 Loading program on the PD DAS and get ready for the PD detection and monitoring.



```
20.000 , [ max MHz= 730.842 , max dBm= -83.052 ] ...noise  
cumulative: 72927, current: 999 >>> cf MHz= 750.000 , span MHz=  
20.000 , [ max MHz= 754.108 , max dBm= -86.612 ] ...noise  
cumulative: 73926, current: 999 >>> cf MHz= 760.000 , span MHz=  
20.000 , [ max MHz= 767.996 , max dBm= -35.704 ] ...THRESHOLD  
cumulative: 74925, current: 999 >>> cf MHz= 770.000 , span MHz=  
20.000 , [ max MHz= 767.996 , max dBm= -35.814 ] ...THRESHOLD  
cumulative: 75924, current: 999 >>> cf MHz= 780.000 , span MHz=  
20.000 , [ max MHz= 786.693 , max dBm= -88.017 ] ...noise  
cumulative: 76923, current: 999 >>> cf MHz= 790.000 , span MHz=  
20.000 , [ max MHz= 797.595 , max dBm= -85.941 ] ...noise  
cumulative: 77922, current: 999 >>> cf MHz= 800.000 , span MHz=  
20.000 , [ max MHz= 803.607 , max dBm= -84.769 ] ...noise  
cumulative: 78921, current: 999 >>> cf MHz= 810.000 , span MHz=  
20.000 , [ max MHz= 811.343 , max dBm= -84.639 ] ...noise
```

Figure 15 Capturing signals above the preset power threshold.

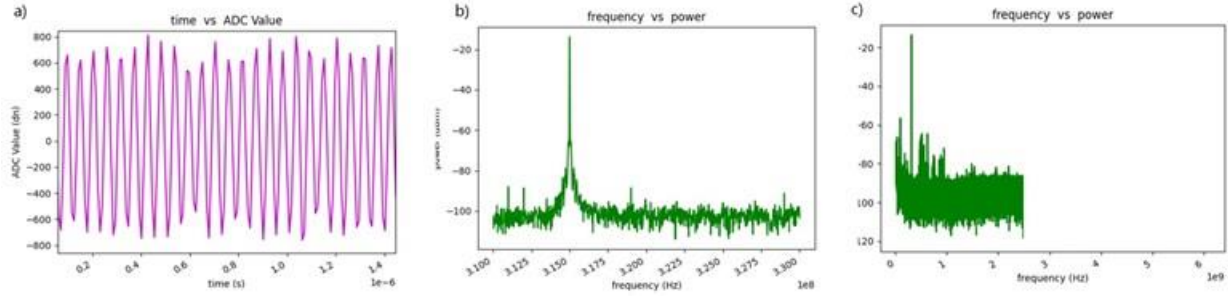


Figure 16 Capturing 315MHz RF/PD signals a) I/Q ADC values in time domain, b) impulse at 315MHz in frequency domain for one frame, c) impulse at 315MHz in complete scanning iteration

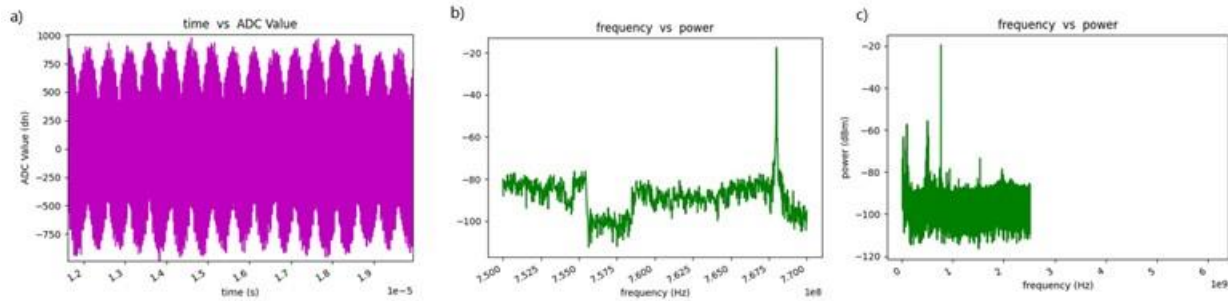


Figure 17 Capturing 768MHz RF/PD signals a) I/Q ADC values in time domain, b) impulse at 768MHz in frequency domain for one frame, c) impulse at 768MHz in complete scanning iteration

### 3.3 Dual/Multiple RF/PD Signal Capturing

We also have run the dual RF/PD detection test to confirm that if multiple PD events occur approximately at the same time (i.e., in one scanning iteration), the PD DAS can capture both of them. We first create a Bluetooth signal (i.e., about 2400 MHz) by turning on two Bluetooth devices and transmitting large files from one device to the other. Meanwhile, we create another 768 MHz signal with AWG as aforementioned, and turn on the PD DAS. It is worth noting that we have to adjust the RF/PD detection threshold to -70dB so as to catch the low power Bluetooth signal. As depicted in Figure 18, one can see that the DAS can clearly capture both 768MHz and the Bluetooth signals.

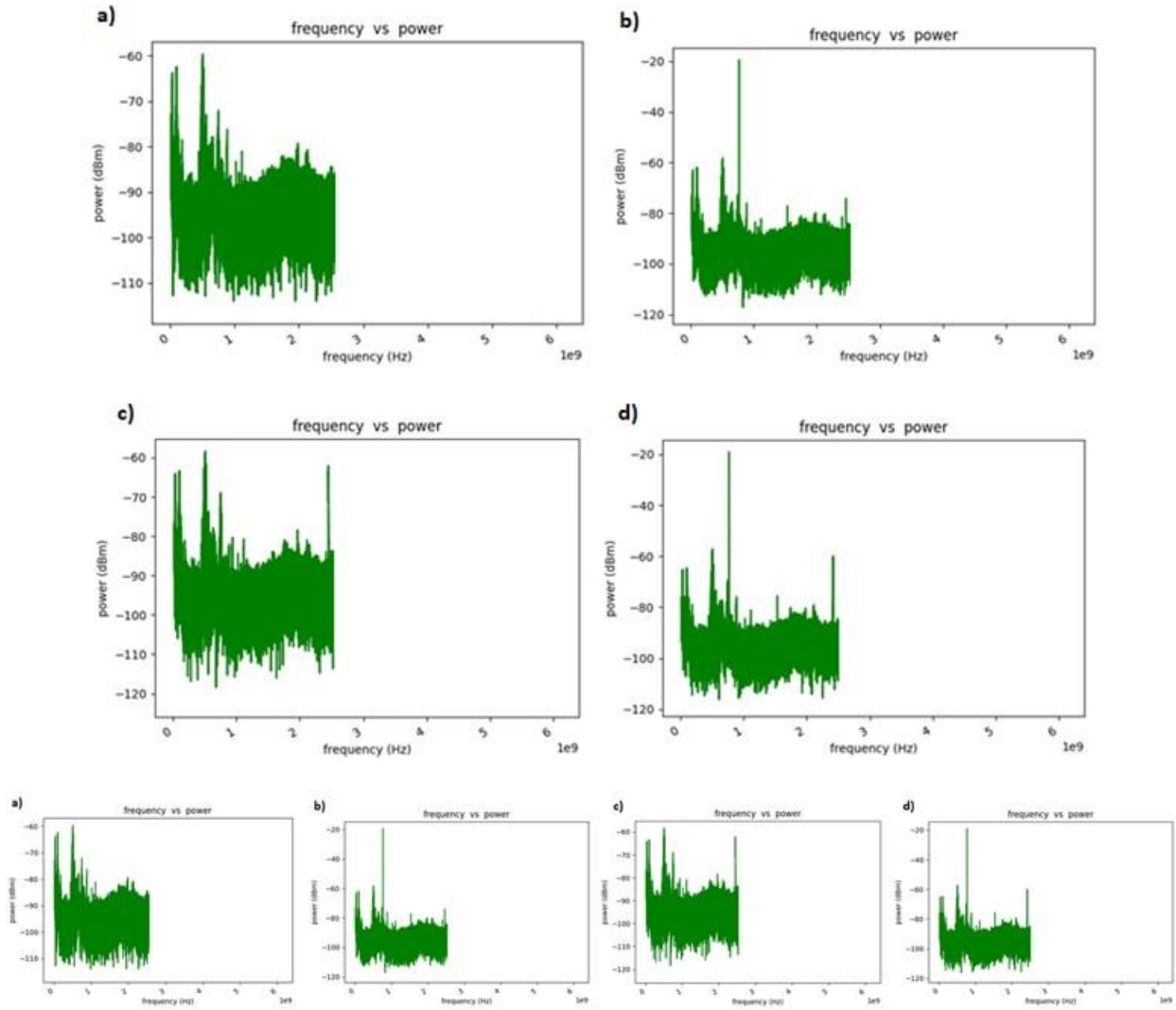


Figure 18 a) No test signal generated (only noises), b) only with a 768MHz generated by AWG, c) only with a Bluetooth signal at about 2400MHz, d) with both 768MHz and Bluetooth signals in the air.

### 3.4 Cloud-Cased Remote Monitoring

The cloud service is established on the DAS via Google drive and Rclone, so that any files created and edited within this particular Google drive folder will be automatically synchronized in all terminals that use the same Google drive account. Once the user logs in with proper credentials (Figure 19.a) on a remote device (e.g., a smartphone), one can see the updated I/Q data and spectrum diagrams (Figure 19.b), and corresponding file attribute details (Figure 19.c). In addition to the real-time synchronization from the local PD DAS to the cloud and granting remote accessibility, the cloud also sends a notification email to the user whenever any new PD signals are detected (Figure 20). In that case, personnel who is in charge of monitoring the switchgears and transformers in high-speed rail can be alerted at early stage to minimize the potential damage and maintenance cost PD may cause.

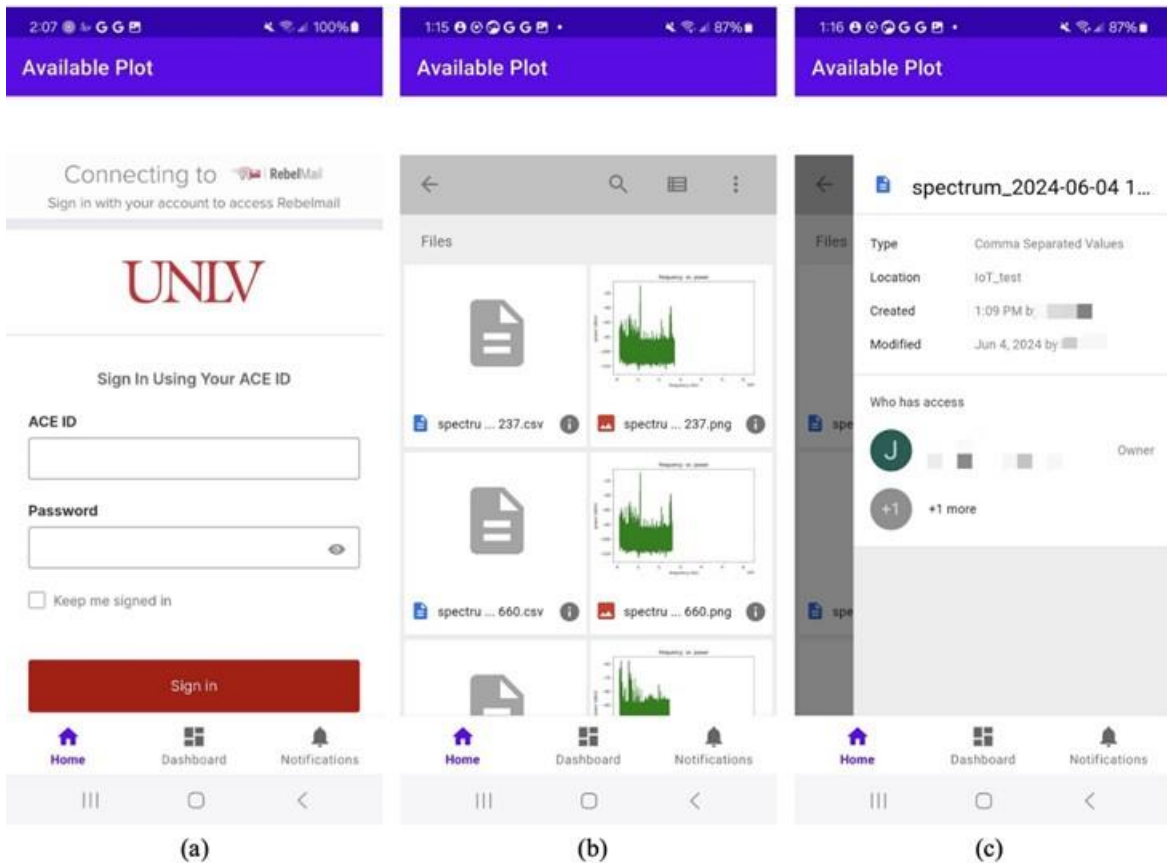


Figure 19 a) APP login, b) APP access to files, c) File attribute details

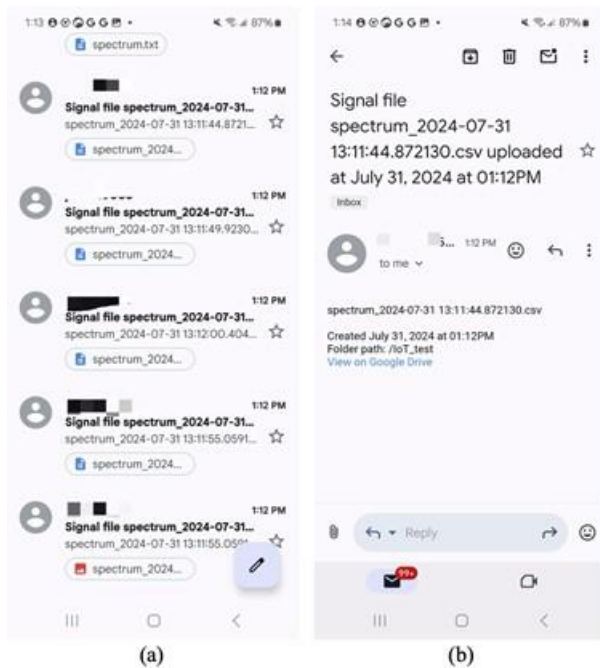


Figure 20 Email notification of detecting new PD signals

## CHAPTER 4 - CONCLUSIONS

This study has successfully developed an advanced platform for the non-disruptive, continuous, real-time detection and monitoring of partial discharges (PD) in switchgears and transformers used within high-speed rail infrastructure. The system is designed to iteratively scan and capture PD signals within a frequency range of 100MHz to 2500MHz, ensuring comprehensive coverage and detection of PD activities.

In addition to its robust detection capabilities, the system is seamlessly integrated with cloud services, enabling remote accessibility to real-time PD data and analysis results. This feature facilitates prompt decision-making and timely interventions by maintenance teams, significantly enhancing the overall reliability and safety of high-speed rail operations.

Extensive laboratory evaluations have been conducted to assess the system's performance. These evaluations demonstrate the system's effectiveness and proficiency in automated real-time PD detection and long-term monitoring. The results indicate that the platform not only meets but exceeds the operational requirements, ensuring that potential faults are identified and addressed promptly before they can escalate into major issues.

The successful implementation of this platform marks a significant advancement in the maintenance and monitoring of high-voltage electrical infrastructure in high-speed rail systems. By leveraging real-time data and remote monitoring capabilities, this system represents a proactive approach to infrastructure management, reducing the risk of unexpected failures and enhancing the overall efficiency and safety of high-speed rail operations.

### ACKNOWLEDGEMENT

This study was conducted with the support from the USDOT Tier 1 University Transportation Center on Railroad Sustainability and Durability.

We would like to express our sincere gratitude to Dr. Ruixue Sun for his invaluable assistance and insightful comments during the project. We also appreciate Mr. David Nakasone and Jiawei Fan for their technical assistance and efforts in the project.

### REFERENCES

1. Bergmans, J.W.M., 2013. Digital Baseband Transmission and Recording. Springer Science & Business Media.
2. BNC, 2021. Arbitrary Waveform Generator - Model 685 | BNC. URL <https://www.berkeleynucleonics.com/model-685>.
3. California, S. of, 2008. High-Speed Rail in California. California High Speed Rail. URL <https://hsr.ca.gov/high-speed-rail-in-california/>.
4. Campos, J., de Rus, G., 2009. Some stylized facts about high-speed rail: A review of HSR experiences around the world. Transport Policy 16, 19–28. <https://doi.org/10.1016/j.tranpol.2009.02.008>
5. Craig-Wood, N., 2014. Rclone. URL <https://rclone.org/>

6. Davies, N., 2009. Partial Discharge (PD) techniques for measuring the condition of ageing HV/MV switchgear.
7. Douglas, H., Roberts, C., Hillmansen, S., Schmid, F., 2015. An assessment of available measures to reduce traction energy use in railway networks. *Energy Conversion and Management* 106, 1149–1165. <https://doi.org/10.1016/j.enconman.2015.10.053>
8. Feng, D., Lin, S., He, Z., Sun, X., 2017. A technical framework of PHM and active maintenance for modern high-speed railway traction power supply systems. *International Journal of Rail Transportation* 5, 145–169. <https://doi.org/10.1080/23248378.2017.1286954>
9. F.H. Kreuger, 1989. *Partial discharge detection in high-voltage equipment*. Butterworth.
10. Fox, W., Vranich, J., Moore, A.T., 2008. *California High Speed Rail Proposal: A Due Diligence Report*.
11. Gast, M., 2005. *802.11 Wireless Networks: The Definitive Guide*. O'Reilly Media, Inc.
12. Giussani, R., Cotton, I., Sloan, R., 2012. Comparison of IEC 60270 and RF partial discharge detection in an electromagnetic noise-free environment at differing pressures, in: *2012 IEEE International Symposium on Electrical Insulation*. Presented at the 2012 IEEE International Symposium on Electrical Insulation, pp. 127–131. <https://doi.org/10.1109/ELINSL.2012.6251441>
13. Givoni, M., 2006. Development and Impact of the Modern High-speed Train: A Review. *Transport Reviews* 26, 593–611. <https://doi.org/10.1080/01441640600589319>
14. Hauschild, W., Lemke, E., 2019. *High-Voltage Test and Measuring Techniques*. Springer International Publishing, Cham. <https://doi.org/10.1007/978-3-319-97460-6>
15. Hussain, M.M., Farokhi, S., McMeekin, S.G., Farzaneh, M., 2016. Prediction of surface degradation of composite insulators using PD measurement in cold fog, in: *2016 IEEE International Conference on Dielectrics (ICD)*. Presented at the 2016 IEEE International Conference on Dielectrics (ICD), pp. 697–700. <https://doi.org/10.1109/ICD.2016.7547711>
16. IEC, 2014. *High-voltage switchgear and controlgear - Part 211: Direct connection between power transformers and gas-insulated metal-enclosed switchgear for rated voltages above 52 kV*.
17. IEEE, 2024. *IEEE Recommended Practice for Partial Discharge Measurement in Liquid-Filled Power Transformers and Shunt Reactors*. IEEE Std C57.113-2023 (Revision of IEEE Std C57.113-2010) 1–45. <https://doi.org/10.1109/IEEESTD.2024.10471340>
18. Jahangir, H., Akbari, A., Werle, P., Szczechowski, J., 2017. Possibility of PD calibration on power transformers using UHF probes. *IEEE Transactions on Dielectrics and Electrical Insulation* 24, 2968–2976. <https://doi.org/10.1109/TDEI.2017.006374>
19. Judd, M.D., 2011. Experience with UHF partial discharge detection and location in power transformers, in: *2011 Electrical Insulation Conference (EIC)*. Presented at the 2011 Electrical Insulation Conference (EIC), pp. 201–205. <https://doi.org/10.1109/EIC.2011.5996146>
20. Judd, M.D., Yang, L., Hunter, I.B.B., 2005a. Partial discharge monitoring of power transformers using UHF sensors. Part I: sensors and signal interpretation. *IEEE Electrical Insulation Magazine* 21, 5–14. <https://doi.org/10.1109/MEI.2005.1412214>
21. Judd, M.D., Yang, L., Hunter, I.B.B., 2005b. Partial discharge monitoring for power transformer using UHF sensors. Part 2: field experience. *IEEE Electrical Insulation Magazine* 21, 5–13. <https://doi.org/10.1109/MEI.2005.1437603>
22. Jürgen Fabian, Martin Neuwersch, Christof Sumereder, Michael Muhr, Robert Schwarz, 2014. State of the Art and Future Trends of Unconventional PD-Measurement at Power Transformers. *JEPE* 8. <https://doi.org/10.17265/1934-8975/2014.06.015>
23. Kim, D., Sampath, U., Kim, H., Song, M., 2017. A fiber-optic multi-stress monitoring system for power transformer, in: *2017 25th Optical Fiber Sensors Conference (OFS)*. Presented at the 2017 25th Optical Fiber Sensors Conference (OFS), pp. 1–4. <https://doi.org/10.1117/12.2265676>

24. Kim, Y.-J., Hikita, M., 2013. A proposal for Hybrid PD sensor identifying absolute distance from PD source, in: 2013 Annual Report Conference on Electrical Insulation and Dielectric Phenomena. Presented at the 2013 Annual Report Conference on Electrical Insulation and Dielectric Phenomena, pp. 1177–1180. <https://doi.org/10.1109/CEIDP.2013.6748319>
25. Kraetge, A., Hoek, S., Koch, M., Koltunowicz, W., 2013. Robust measurement, monitoring and analysis of partial discharges in transformers and other HV apparatus. *IEEE Transactions on Dielectrics and Electrical Insulation* 20, 2043–2051. <https://doi.org/10.1109/TDEI.2013.6678852>
26. Kučera, M., Jarina, R., Brnčal, P., Gutten, M., 2019. Visualisation and Measurement of Acoustic Emission from Power Transformers, in: 2019 12th International Conference on Measurement. Presented at the 2019 12th International Conference on Measurement, pp. 303–306. <https://doi.org/10.23919/MEASUREMENT47340.2019.8779880>
27. Ma, G.-M., Li, C.-R., Mu, R.-D., Jiang, J., Luo, Y.-T., 2014. Fiber bragg grating sensor for hydrogen detection in power transformers. *IEEE Transactions on Dielectrics and Electrical Insulation* 21, 380–385. <https://doi.org/10.1109/TDEI.2013.004381>
28. Paoletti, G., Baier, M., 2001. Failure contributors of MV electrical equipment and condition assessment program development, in: Conference Record of 2001 Annual Pulp and Paper Industry Technical Conference (Cat. No.01CH37209). Presented at the Conference Record of 2001 Annual Pulp and Paper Industry Technical Conference (Cat. No.01CH37209), pp. 37–47. <https://doi.org/10.1109/PAPCON.2001.952946>
29. Qian, S., Chen, H., Xu, Y., Su, L., 2018. High sensitivity detection of partial discharge acoustic emission within power transformer by sagnac fiber optic sensor. *IEEE Transactions on Dielectrics and Electrical Insulation* 25, 2313–2320. <https://doi.org/10.1109/TDEI.2018.007131>
30. Sarkar, B., Koley, C., Roy, N.K., Kumbhakar, P., 2015. Condition monitoring of high voltage transformers using Fiber Bragg Grating Sensor. *Measurement* 74, 255–267. <https://doi.org/10.1016/j.measur.2015.08.016>
31. Sheng, J., Wu, G., LaishengTong, LijunZhou, JunZhang, 2004. Study on gas and oil separating plant used for online monitoring system of transformer, in: Conference Record of the 2004 IEEE International Symposium on Electrical Insulation. Presented at the Conference Record of the 2004 IEEE International Symposium on Electrical Insulation, pp. 93–96. <https://doi.org/10.1109/ELINSL.2004.1380467>
32. Sibal, V., 2010. Technical Memorandum: Traction Power Facilities, General Standardization Requirements. California High-Speed Rail Authority.
33. Skelly, D., 2012. Photo-acoustic spectroscopy for dissolved gas analysis: Benefits and Experience, in: 2012 IEEE International Conference on Condition Monitoring and Diagnosis. Presented at the 2012 IEEE International Conference on Condition Monitoring and Diagnosis, pp. 29–43. <https://doi.org/10.1109/CMD.2012.6416446>
34. Sparkman, O.D., Penton, Z., Kitson, F.G., 2011. *Gas Chromatography and Mass Spectrometry: A Practical Guide*. Academic Press.
35. Tektronix, 2020. 5 Series B MSO Mixed Signal 8 Channel Oscilloscope. URL <https://www.tek.com/en/products/oscilloscopes/5-series-mso>.
36. Tektronix, 2017. RSA306, RSA306B, and RSA500A/600A Series Spectrum Analyzers Application Programming Interface (API) Programming Reference.
37. Tektronix, R., 2015. RSA306B USB Real Time RF Spectrum Analyzer. URL <https://www.tek.com/en/products/spectrum-analyzers/rsa306>.
38. Tenbohlen, S., Beltle, M., Siegel, M., 2017. PD monitoring of power transformers by UHF sensors, in: 2017 International Symposium on Electrical Insulating Materials (ISEIM). Presented at the 2017 International Symposium on Electrical Insulating Materials (ISEIM), pp. 303–306. <https://doi.org/10.23919/ISEIM.2017.8088747>



39. Timperley, J.E., 1983. Incipient Fault Identification Through Neutral RF Monitoring of Large Rotating Machines. *IEEE Transactions on Power Apparatus and Systems PAS-102*, 693–698. <https://doi.org/10.1109/TPAS.1983.318030>
40. Whitaker, J.C., 2017. *The RF Transmission Systems Handbook*. CRC Press.
41. Yongfen, L., Xiaohu, X., Fei, D., Xiao, T., Yanming, L., 2015. Comparison of DOA Algorithms Applied to Ultrasonic Arrays for PD Location in Oil. *IEEE Sensors Journal* 15, 2316–2323. <https://doi.org/10.1109/JSEN.2014.2374182>

## **ACKNOWLEDGEMENTS**

This study was conducted with the support from the USDOT Tier 1 University Transportation Center on Railroad Sustainability and Durability.

## ABOUT THE AUTHORS

**Dr. Ming Zhu** is the Electrical Engineering Laboratory Director of the Department of Electrical and Computer Engineering at the University of Nevada Las Vegas. His research interests include circuits and VLSI design, robotics and automation, AI/machine learning algorithms and applications, computer and network architectures, computation algorithms and system design. He has a Ph.D. in Electrical Engineering from the University of Nevada Las Vegas.

**Dr. Yingtao Jiang** is a professor in the Department of Electrical and Computer Engineering at the University of Nevada, Las Vegas. His research interests include semiconductors, microelectronics, computer-aided design, unmanned vehicle systems and applications, AI/machine learning algorithms and applications, sensors and instrumentations, computer architectures, wireless communications and STEM education. He has a Ph.D. in Computer Science from the University of Texas at Dallas.